XMM–Newton discovery of very high obscuration in the candidate supergiant fast X-ray transient AX J1714.1−3912

L. Sidoli [1]★ V. Sguera [2] P. Esposito [1,3] L. Oskinova[4,5] and M. Polletta [1]

[1]*INAF, Istituto di Astrofisica Spaziale e Fisica Cosmica, Via A. Corti 12, I-20133 Milano, Italy*
[2]*INAF, Osservatorio di Astrofisica e Scienza dello Spazio, Via P. Gobetti 101, I-40129 Bologna, Italy*
[3]*Scuola Universitaria Superiore IUSS Pavia, Piazza della Vittoria 15, I-27100, Pavia, Italy*
[4]*Institute for Physics and Astronomy, University Potsdam, D-14476 Potsdam, Germany*
[5]*Kazan Federal University, Kremlyovskaya 18, 420008 Kazan, Russia*

ABSTRACT

We have analysed an archival *XMM–Newton* EPIC observation that serendipitously covered the sky position of a variable X-ray source AX J1714.1−3912, previously suggested to be a supergiant fast X-ray transient (SFXT). During the *XMM–Newton* observation the source is variable on a time-scale of hundred seconds and shows two luminosity states, with a flaring activity followed by unflared emission, with a variability amplitude of a factor of about 50. We have discovered an intense iron emission line with a centroid energy of 6.4 keV in the power law-like spectrum, modified by a large absorption ($N_H \sim 10^{24}$ cm^{-2}), never observed before from this source. This X-ray spectrum is unusual for an SFXT, but resembles the so-called 'highly obscured sources', high mass X-ray binaries (HMXBs) hosting an evolved B[e] supergiant companion (sgB[e]). This might suggest that AX J1714.1−3912 is a new member of this rare type of HMXBs, which includes IGR J16318-4848 and CI Camelopardalis. Increasing this small population of sources would be remarkable, as they represent an interesting short transition evolutionary stage in the evolution of massive binaries. Nevertheless, AX J1714.1−3912 appears to share X-ray properties of both kinds of HMXBs (SFXT versus sgB[e] HMXB). Therefore, further investigations of the companion star are needed to disentangle the two hypothesis.

Key words: X-rays: binaries – X-rays: individual: AX J1714.1−3912.

1 INTRODUCTION

One of the legacies of every X-ray mission is the production of source catalogs. They always include a significant fraction of unidentified sources, whose nature remains unknown or controversial for several years, awaiting further investigations. This is the case of AX J1714.1−3912, a source discovered during *ASCA* observations (performed in 1996) of the Galactic supernova remnant (SNR) RX J1713.7 − 3946 (Uchiyama, Takahashi & Aharonian 2002), a shell-like SNR site of production of synchrotron X-ray emission (Koyama et al. 1997; Slane et al. 1999). AX J1714.1−3912 is located beyond the northern rim of the shell, and at first it was suggested to be associated with a molecular cloud (Uchiyama et al. 2002). The *ASCA* spectrum is well modeled by a hard powerlaw with a photon index $\Gamma = 0.98^{+0.44}_{-0.34}$ and an absorbing column density $N_H = 1.28^{+1.00}_{-0.70} \times 10^{22}$ cm^{-2}. This absorption was very similar to the one measured from other regions of the SNR, consistent with the total Galactic one in the source direction ($N_H = 1.5 \times 10^{22}$ cm^{-2}; HI4PI Collaboration et al. 2016). The absorption-corrected flux was 4×10^{-11} erg cm^{-2} s^{-1}(1–10 keV). Given the spatial overlap of the *ASCA* source with the cloud, Uchiyama et al. (2002) interpreted the flat X-ray spectrum as produced by non-thermal bremsstrahlung from particles accelerated in the SNR, then impacting the molecular

gas as a target. This hypothesis assumes the physical proximity of the SNR with the molecular cloud, and that AX J1714.1−3912 is an extended X-ray source.

An observation performed in 2015 with the *Chandra* telescope proved the point-like character of AX J1714.1−3912 (named CXOU J171343.9 − 391205, Miceli & Bamba 2018), excluding the association with the molecular cloud. A relatively low X-ray flux was observed, 7(±3) × 10^{-14} erg cm^{-2} s^{-1} (2–10 keV; corrected for the absorption). Miceli & Bamba (2018) reported also on a *Suzaku* observation of the field containing AX J1714.1 − 3912 performed in 2011, where the source showed a variable X-ray emission, with a short (∼2 ks) hard X-ray flare. The separate spectroscopy of the quiescent emission and the flare resulted into a quite high absorption (N_H in the range 3.6–12.2 × 10^{22} cm^{-2} for emission in quiescence, and $N_H = 6 - 11 \times 10^{22}$ cm^{-2} during the flare) and flat power law spectra (photon index, Γ, in the range 0.6–2.3 during quiescence, and Γ ranging from 0.7 to 1.6 during the flare, at 90 per cent confidence level). The observed (not corrected for the absorption) fluxes (2–10 keV) were F = 6 × 10^{-13} erg cm^{-2} s^{-1} and F = 3.6 × 10^{-12} erg cm^{-2} s^{-1} for the quiescent and flare emission, respectively.

On this basis, Miceli & Bamba (2018) proposed that AX J1714.1−3912 is a high mass X-ray binary (HMXB) belonging to the sub-class of the supergiant fast X-ray transients (SFXTs; Sguera et al. 2005, 2006; Negueruela et al. 2006). The positional overlap with the near-infrared (NIR) point source 2MASS


★ E-mail: lara.sidoli@inaf.it
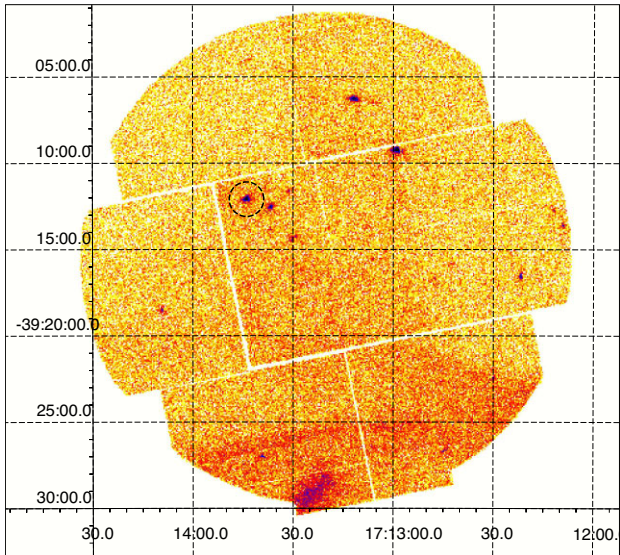
Figure 1. EPIC MOS2 image of the *XMM–Newton* observation of the northern region of the SNR RX J1713.7 − 3946. The sky position of AX J1714.1−3912 is marked with the black, dashed circle. The northern rim of the SNR shell is evident in the lowest part of the image.

17134391-3912055 further supported the identification with a massive X-ray binary (Miceli & Bamba 2018).

2 OBSERVATIONS AND DATA ANALYSIS

The sky position of AX J1714.1−3912 was serendipitously covered by *XMM–Newton* (Jansen et al. 2001) during an observation performed in 2017, from August 29 (at 15:28, UTC) to August 30 (at 04:08), with an on-time exposure of 41.6 ks (pn) and 45.5 ks (MOS). The observation (Obs.ID 0804300901) was targeted at the northern region of the SNR RX J1713.7 − 3946 and imaged AX J1714.1−3912 at an offaxis angle of about 5 arcmin. In Fig. 1, we show the MOS2 field-of-view , where AX J1714.1−3912 is marked by a dashed black circle.

The three European Photon Imaging Cameras (EPIC) (Strüder et al. 2001; Turner et al. 2001) operated with the medium filter, with the pn in full frame extended window, and the two MOS in full frame mode. EPIC data were reprocessed using the version 18 of the *XMM–Newton* Science Analysis Software (SAS), with standard procedures. The tools RMFGEN and ARFGEN, available in the SAS, were used to generate the response and ancillary matrices, respectively. High background levels were filtered-out before extracting EPIC spectra. Light curves and spectra were extracted from circles centered on the source emission, adopting a 30 arcsec radius, selecting patterns from 0 to 4 (EPIC pn), and from 0 to 12 (MOS). Similar size regions, offset from the source position but lying on the same CCD, were used to extract background spectra. Source spectra from the pn, MOS1 and MOS2 were simultaneously fitted using XSPEC (version 12.10.1; Arnaud 1996) in the energy range 0.3–12 keV, allowing for free cross-calibration constants, to take into account calibration uncertainties. All fluxes were estimated in the 1–10 keV range. The models TBABS and TBPCF were adopted to account for the absorbing column density along the line of sight, assuming the photoelectric absorption cross sections of Verner et al. (1996) and the interstellar abundances of Wilms, Allen & McCray (2000). The spectra were rebinned to have at least 20 counts per
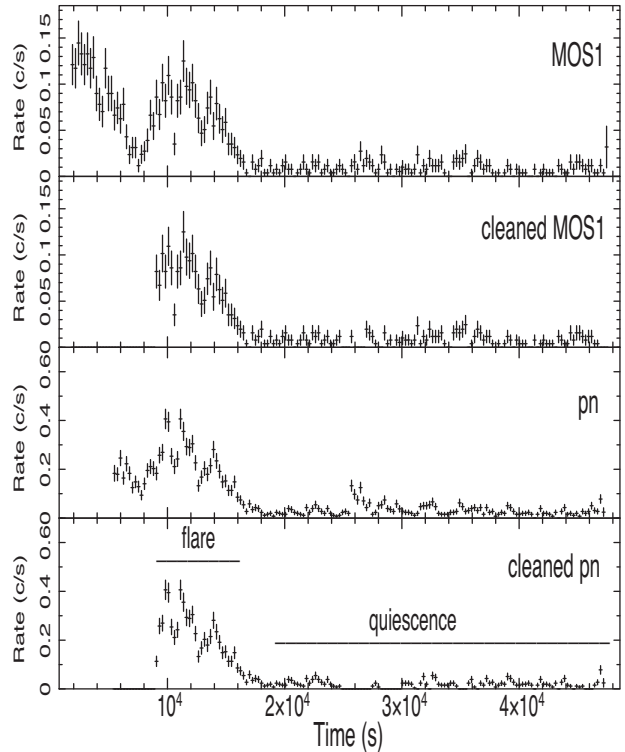
Figure 2. AX J1714.1−3912 light curve in the energy band 0.3–12 keV (bin time = 256 s) observed by *XMM–Newton*. From top to bottom, we show the MOS1 source light curve (MOS2 one is similar), the cleaned MOS1 one (where time intervals with high background levels have been filtered-out), the EPIC pn light curve and the cleaned one (lowest panel). The horizontal lines in the lowest panel indicate the time intervals for the extraction of the flare and quiescent EPIC spectra (the same for pn, MOS1, and MOS2).

bin, to apply the χ^2 statistics. All uncertainties are computed at 90 per cent confidence level, for one interesting parameter. The uncertainty on the X-ray fluxes have been calculated using CFLUX in XSPEC.

3 RESULTS

3.1 Temporal analysis

The EPIC source light curve is reported in Fig. 2, before and after filtering for high background levels. The source displays a significant variability on time-scales of a few hundred seconds, with a dynamic range of ∼50. Although formally the energy range is 0.3–12 keV, we note that most of the source counts lies in the 2–12 keV energy band. We have identified two source states: a high state (or 'flare', hereafter) and a low one, named 'quiescence', indicated in the lowest panel in Fig. 2.

We searched the data for periodic signals by means of Fourier transforms and Rayleigh periodograms, but we did not find any statistically significant signal. The 3σ upper limit on the pulsed fraction, computed by extensive Monte Carlo simulations, is 25 per cent for a sinusoidal signal between 0.4 and 5.4 s, using only the pn data (2–12 keV), and 20 per cent between 5.4 and 1000 s, using also the data from the MOS cameras. Above ≈1000 s, the strong red noise does not allow us to set meaningful limits.
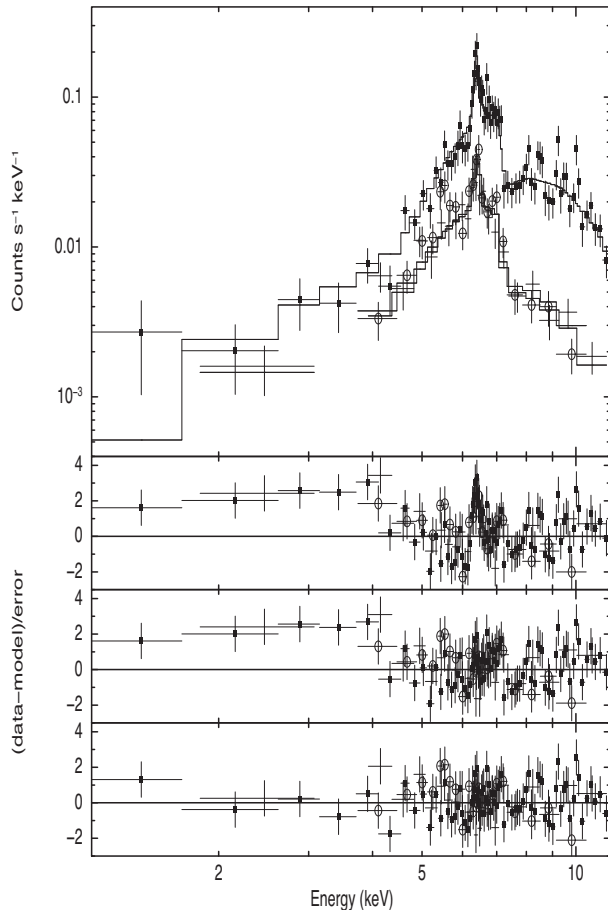
Figure 3. EPIC spectra extracted during the flare. Counts spectra are shown in the top panel (EPIC pn is marked with solid squares, MOS1 with open circles, MOS2 with crosses), when fitted with the best fit reported in Table 1. Residuals (in units of standard deviation) with respect to three models are shown in the bottom panel: from top to bottom, the residuals are with respect to a single absorbed powerlaw, with respect to a powerlaw with a Gaussian line at 6.4 keV, and including a partial covering absorption model (i.e. the best fit reported in Table 1).

3.2 Spectroscopy

We performed the spectroscopic analysis during the flare and in quiescence separately, extracting two sets of EPIC spectra, covering the time intervals shown in Fig. 2 (bottom panel). The EPIC spectra extracted during the flare are highly absorbed and with large positive residuals around 6.4 keV, very evident when fitting the spectra with a simple, absorbed power law model (Fig. 3), resulting in a reduced $\chi^2_\nu = 1.928$ (for 117 degrees of freedom, dof; see Table 1 for the spectral parameters). The addition of a narrow Gaussian line accounted for these residuals (χ^2_ν/dof = 1.445/114; Table 1). However, a mild soft excess remained below 4 keV. This suggested to consider an additional absorption model, a partial covering fraction absorption (TBPCF in XSPEC), where the additional column density is applied to a fraction of the power law emission. This final model provides a good description of the flare spectrum (Model 3 in Table 1). The counts spectra and the residuals to this best-fitting model are shown in Fig. 3.

We note that the model TBPCF resulted into an almost complete covering (98 ± 1 per cent) of the X-ray emission, leading to an absorption of $1.5 \times 10^{24}\,\mathrm{cm}^{-2}$ during the flare, considering both

absorbing components (TBABS and TBPCF). This is 2 dex larger than the Galactic absorption ($N_H = 1.5 \times 10^{22}\,\mathrm{cm}^{-2}$; HI4PI Collaboration et al. 2016). The centroid of the emission line is very well constrained in a narrow range around 6.4 keV in both states, clearly indicative of fluorescence from neutral iron.

The Fe K_α line is produced when a direct hard X-ray radiation illuminates neutral matter around the source. This reprocessing results into a fluorescent iron line emission together with a Compton component. The final spectrum is a composition of a reflection component together with the direct (power law) X-ray emission. However, adopting reflection models like PEXRAV (Magdziarz & Zdziarski 1995) and PEXMON (Nandra et al. 2007) in XSPEC did not yield better fits. We note that disentangling the incident and the reflected component is made difficult due to the limited energy band and the low counting statistics. This results into a quite hard power law slope measured in the total spectrum below 10 keV, also because of a reflected hump (Fabian et al. 1990) that is expected beyond the *XMM–Newton* energy band.

The spectrum in quiescence shows a prominent positive excess around 6.4 keV as well, when fitted with a simple absorbed power law (χ^2_ν/dof = 2.85/6). The addition of a Gaussian line to the absorbed power law model resulted in a good fit to the data, with no need to adopt further partial covering absorption (Fig. 4). During the fit, a narrow iron emission line is assumed, fixing its width to zero. The best-fitting parameters are listed in Table 1 (last column).

4 DISCUSSION

We have reported on the discovery of a prominent FeKα line and a large intrinsic absorption ($N_H = 1.5 \times 10^{24}\,\mathrm{cm}^{-2}$) from AX J1714.1−3912 during an *XMM–Newton* observation performed in 2017. The source shows a variable X-ray emission with a brighter state (flare) at the beginning of the observation, followed by a fainter state (quiescence). Spectra extracted from both states are well described by hard power law models with similar slopes, within the uncertainties. The X-ray emission is significantly more absorbed during the flare than during the following fainter state, suggesting a variability in the circumstellar absorbing matter on short time-scale, correlated with the X-ray flux.
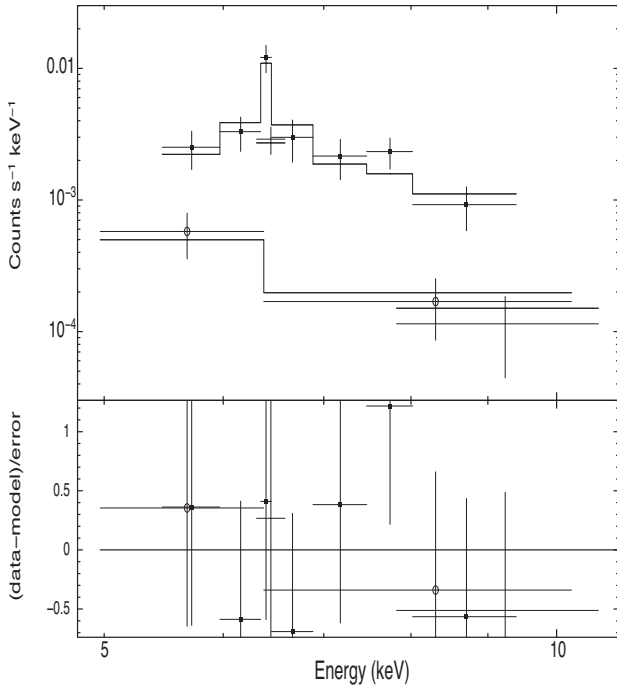
The FeKα is detected in both states, with a larger equivalent width during the quiescent emission. This might suggest that the unflared state is due to the eclipse by the companion star: the less absorbed X-ray spectrum can be due to scattering into the line of sight by the stellar wind matter of the central (eclipsed) X-ray radiation (e.g. Haberl 1991). However, the flux of the iron line is significantly different in the two states and correlates with the continuum flux, disfavouring this hypothesis, and suggests an intrinsic variability. Moreover, this correlation indicates a close proximity of the reprocessing matter to the compact object.

The source is also variable on long time-scales of years: previous X-ray observations (*ASCA* in 1996, *Suzaku* in 2011, *Chandra* in 2015) caught different X-ray fluxes (Fig. 5) and a significantly lower absorbing column density (N_H in the range 10^{22}–$^{23}\,\mathrm{cm}^{-2}$) than during the *XMM–Newton* observation. This indicates a long-term changing aspect of the absorbing matter local to the source, possibly with an inhomogeneous distribution or a variability due to the orbital motion in a binary system.

In light of the new *XMM–Newton* results, we discuss the possible source nature in the following subsections.

Table 1. Spectroscopy of the two source states (EPIC pn, MOS1, and MOS2). We show spectral results obtained using three models for the flare emission: Model 1 is a simple absorbed power law, Model 2 includes an iron line in emission, while the best-fitting model is Model 3, a partially absorbed powerlaw, together with a Gaussian line in emission [CONST ∗ TBABS ∗ TBPCF ∗ (POW + GAU) in XSPEC synthax]. The last column lists the best-fitting parameters for the spectroscopy during quiescence [CONST ∗ TBABS ∗ (POW + GAU)]. $F_{1-10keV}$ is the absorbed flux, $UF_{1-10keV}$ the flux corrected for the absorption.

Parameters	Flare			Quiescence
	Model 1	Model 2	Model 3	
N_H (10^{22} cm^{-2})	127^{+16}_{-15}	99^{+18}_{-17}	$5.8^{+6.3}_{-4.0}$	<80
—— Partial covering fraction absorption ——				
N_{HTBpcf} (10^{22} cm^{-2})	–	–	145 ± 20	–
Covering fraction	–	–	98 ± 1 per cent	–
—— POWER LAW——				
Γ	$0.21^{+0.32}_{-0.32}$	$-0.40^{+0.39}_{-0.39}$	$0.06^{+0.37}_{-0.38}$	$-0.8^{+1.6}_{-1.7}$
Norm	$10(^{+12}_{-6}) \times 10^{-4}$	$2.0(^{+3.3}_{-1.2}) \times 10^{-4}$	$8.4(^{+13.5}_{-5.3}) \times 10^{-4}$	$1.1(^{+50}_{-1.0}) \times 10^{-6}$
—— GAUSSIAN LINE——				
E_{line} (keV)	–	$6.409^{+0.025}_{-0.027}$	$6.402^{+0.024}_{-0.026}$	$6.41^{+0.06}_{-0.05}$
σ (keV)	–	<0.10	<0.08	0.0 (fixed)
Norm (photons cm^{-2} s^{-1})	–	$1.3^{+0.4}_{-0.3} \times 10^{-4}$	$2.0^{+0.7}_{-0.5} \times 10^{-4}$	$4.4^{+6.3}_{-1.8} \times 10^{-6}$
EW (eV)	–	320^{+80}_{-70}	265^{+30}_{-80}	900^{+1300}_{-400}
$F_{1-10keV}$ (erg cm^{-2} s^{-1})	$9.2 \pm 0.5 \times 10^{-12}$	$9.3 \pm 0.5 \times 10^{-12}$	$9.4 \pm 0.5 \times 10^{-12}$	$4.3^{+0.9}_{-1.2} \times 10^{-13}$
$UF_{1-10keV}$ (erg cm^{-2} s^{-1})	$5.4^{+1.6}_{-1.2} \times 10^{-11}$	$3.4^{+1.1}_{-0.8} \times 10^{-11}$	$6.2^{+2.5}_{-1.7} \times 10^{-11}$	$4.4^{+3.1}_{-0.1} \times 10^{-13}$
$L_{1-10keV}$ (erg s^{-1})	6.5×10^{35} d^2_{10kpc}	4.1×10^{35} d^2_{10kpc}	7.4×10^{35} d^2_{10kpc}	5.3×10^{33} d^2_{10kpc}
χ^2_ν/dof	1.928/117	1.445/114	1.076/112	0.854/4

Figure 4. EPIC spectra extracted during quiescence. Counts spectra are shown in the top panel (EPIC pn is marked with solid squares, MOS1 with open circles, MOS2 with crosses), when fitted with the best fit reported in Table 1, an absorbed power law together with an emission line at 6.4 keV. The lower panel shows the residuals in units of standard deviation.

4.1 Is AX J1714.1−3912 an active galactic nucleus?

The point-like appearance, the large intrinsic absorption and the presence of an FeKα line in AXJ 1714.1 − 3912 are reminiscent of the X-ray properties of obscured active galactic nuclei (AGN; see e.g.
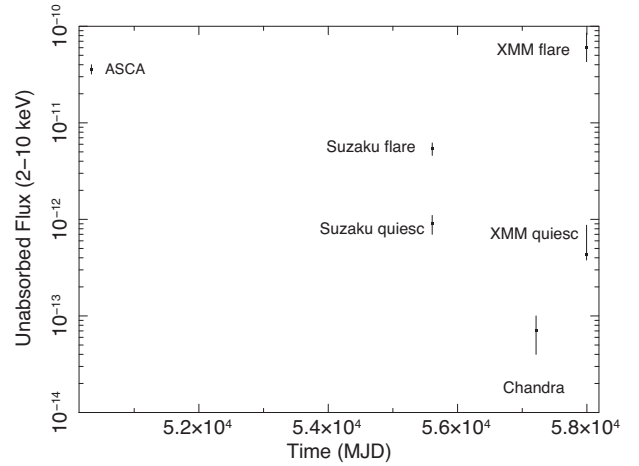
Figure 5. AX J1714.1−3912 long term light curve (fluxes in the energy range 2–10 keV are corrected for the absorption).

Guainazzi, Matt & Perola 2005). To investigate such a hypothesis we examine the broad-band spectral energy distribution (SED) of the optical-infrared (IR) counterpart to AXJ 1714.1 − 3912. To build the broadband SED we collected optical data from GAIA DR3 (Gaia Collaboration et al. 2016, 2021), near-IR data from 2MASS (Skrutskie et al. 2006), and mid-IR data from WISE (Wright et al. 2010) and *Spitzer* (Werner et al. 2004; Benjamin et al. 2003). The optical-IR SED, shown in Fig. 6, peaks at ∼2 μm and decreases steadily towards longer wavelengths up to $\lambda \leq 10 \mu$m. Such a behaviour is inconsistent with what is observed in AGN, whose SEDs typically rise long-ward of 1–5 μm (Polletta et al. 2007; Hickox et al. 2017) due to the emission from AGN-heated hot dust. Therefore, the broad-band SED rules out the AGN hypothesis. The mid-IR ($\lambda = 3$–10 μm) SED of AXJ 1714.1 − 3912 is instead consistent with stellar
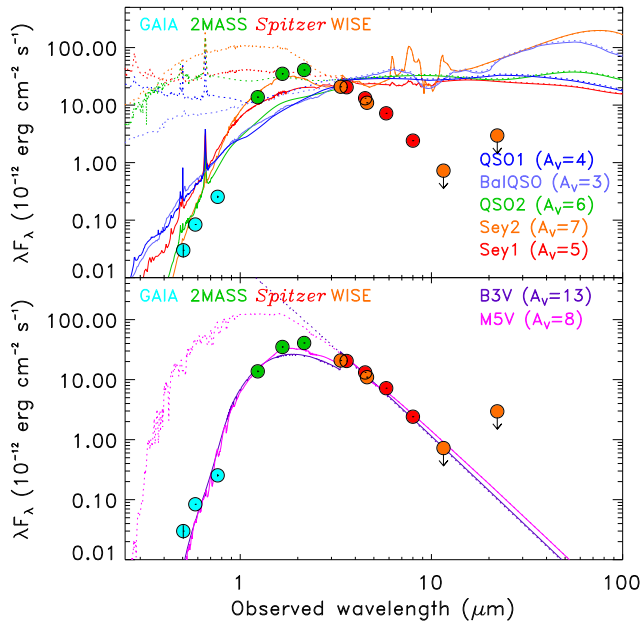
Figure 6. Spectral energy distribution of AX J1714.1 − 3912 (full circles: GAIA in cyan, 2MASS in green, *Spitzer* in red and WISE in orange). The lines represent various templates normalized at the observed 3.6μm flux with no reddening (dotted) or with different amounts of reddening (solid), as annotated, applied to reproduce the observed optical-NIR SED. Templates of various types of AGN are shown in the *top panel* (Polletta et al. 2007), and of a B and M-type star (Kurucz 1993) in the *bottom panel*.

radiation. The full optical-IR SED of AXJ 1714.1 − 3912 can be reproduced with various reddened stellar templates (Kurucz 1993). We apply a standard Galactic reddening law (Cardelli, Clayton & Mathis 1989). The amount of required optical extinction depends on the stellar type, for example an A_V of 13 mag, corresponding to $N_H \simeq 2.3 \times 10^{22}$ cm^{-2}, is required for a B-type star, and an A_V of 8 mag ($N_H \simeq 1.4 \times 10^{22}$ cm^{-2}) for a red-giant M-type star. The estimated column densities are consistent or slightly larger than the Galactic value measured along the line of sight towards AXJ 1714.1 − 3912 (i.e. 1.5×10^{22} cm^{-2}; HI4PI Collaboration et al. 2016). Spectroscopic observations and a more detailed analysis would be necessary to better characterize the stellar type and determine whether intrinsic dust absorption is present in AXJ 1714.1 − 3912.

4.2 Is AX J1714.1−3912 an SFXT?

Miceli & Bamba (2018) excluded an extragalactic origin as well, based on the rapid time-scale (thousands seconds) of the X-ray flux variability. They suggested that AX J1714.1−3912 is a Galactic HMXB belonging to the sub-class of SFXTs, based on the point-like appearence, the amplitude of the X-ray variability and the hard power law spectrum, indicative of accretion of matter on to a compact object.

In light of the flare caught by *XMM–Newton*, the source dynamic range (F_{max}/F_{min}) increases to ∼900, compared with the faint flux detected by *Chandra* (Fig. 5). This range of variability is not as extreme as the one shown by the prototypical members of the SFXT class (F_{max}/F_{min} from 10^4 to 10^6) but still consistent with less variable, 'intermediate' SFXTs (see Table 2 in Sidoli & Paizis 2018). However it is possible that we missed the brightest flares, since the duty cycle of SFXT outbursts is very small (lower than 5 per cent, see Table 1 in Sidoli & Paizis 2018). On the other hand, the source field has been

monitored by *INTEGRAL*/IBIS (above 20 keV) for a total exposure time of 6.7 Ms (Bird et al. 2016), with no detections reported in the literature. If we assume a typical flare duration of ∼2 ks we calculate a duty cycle lower than 0.03 per cent for AX J1714.1−3912 (per centage of time spent in bright flaring activity, i.e. with a peak flux $F_{18-50keV} \geq 1.5–3 \times 10^{-10}$ erg cm^{-2} s^{-1}; Sidoli & Paizis 2018), to reconcile with the lack of reported outbursts with *INTEGRAL*. This would imply that AX J1714.1−3912 is the SFXT with the lowest duty cycle: to date, the SFXT with the rarest outbursts is IGR J08408-4503, showing a duty cycle of 0.09 per cent (Sidoli & Paizis 2018). Alternatively, AX J1714.1−3912 could be located at large distance: a short (duration ∼2 ks) flare with a peak luminosity of ∼10^{36} erg s^{-1} (18–50 keV) implies a source distance d$\gtrsim$8 kpc, to not be detected by *INTEGRAL*.

The non detection with *INTEGRAL* poses also a 3σ upper limit to the persistent (quiescent) emission F<2.3 × 10^{-12} erg cm^{-2} s^{-1} (20–40 keV; Bird et al. 2016). If we assume that the quiescent *XMM–Newton* spectrum is representative of the long-term source state, we can use this upper limit to constrain the presence of a high energy cutoff, despite the large uncertainty in the measured power law slope. In particular, if the true photon index of the quiescent spectrum is Γ ∼0.8, the extrapolation of the power law model at higher energies leads to F=1.3 × 10^{-12} erg cm^{-2} s^{-1} (20–40 keV), with no need for a cutoff. If harder power law photon indexes are assumed, variable cutoff values are needed to reconcile with the *INTEGRAL* upper limit. For instance, for a photon index Γ ∼ −1 in the quiescent spectrum, a cutoff E_{cut} ∼10 keV is needed, to match the upper limit to the 20–40 keV flux (where E_{cut} is the e-folding energy of exponential rolloff in the CUTOFFPL model in XSPEC).

4.3 Is AX J1714.1−3912 a supergiant B[e] HMXB?

Although the long-term X-ray light curve is compatible with an SFXT with very rare outbursts (and/or located at large distance), we note that the *XMM–Newton* spectral properties reported here for the first time are unusual for an SFXT (Martínez-Núñez et al. 2017; Sidoli 2017; Kretschmar et al. 2019): so far, no members of this class are known to be so highly absorbed. Even in the SFXT IGR J18410 − 0535, where an intense flare was suggested to be produced by accretion of a very massive wind clump, the associated absorbing column density was significantly lower (Bozzo et al. 2011). The most extreme absorption among SFXTs has been observed in SAX J1818.6 − 1703 (5 × 10^{23} cm^{-2}; Boon et al. 2016), but it is a unique case. In general, SFXTs show a circumstellar environment less dense than in persistent HMXBs (Kretschmar et al. 2019). We note that large absorbing column densities, variable on time-scales of ten days, have been measured in the Be X-ray transient SXP 1062 (González-Galán et al. 2018) during the decline of the outburst, but with no detection of FeKα line emission.

On the other hand, the AX J1714.1−3912 spectrum observed with *XMM–Newton* strongly resembles those of the so-called 'highly obscured sources' (Walter et al. 2003). The latter are HMXBs where the compact object is enshrouded in a dense circumstellar environment produced by the outflowing matter from an evolved, early type massive star, such as a sgB[e]. In particular, the huge absorbing column density of ∼1.5 × 10^{24} cm^{-2}, we deduce from the flare emission, makes AX J1714.1−3912 one of the most absorbed sources ever observed in our Galaxy, together with IGR J16318-4848 (Ibarra et al. 2007).

SgB[e] stars (Zickgraf et al. 1985; Kraus 2019) are evolved massive stars characterized by disc-like, dusty circumstellar envelopes

fed by dense outflows from the B supergiant. Their optical spectra show a twofold behaviour: broad Balmer emission lines plus narrow emission lines from permitted and forbidden transitions. HMXBs with a supergiant B[e] donor stars are a rare type of X-ray binaries, with CI Camelopardalis (CI Cam, aka XTE J0421 + 560; Bartlett et al. 2013) as a prototype, being the first Galactic sgB[e] star observed during an X-ray outburst whose X-ray luminosity implied a clear binarity nature. Chaty et al. (2019) suggest that sgB[e] HMXBs are at the short evolutionary stage when a binary system is entering a common envelope phase of binary evolution. At present, this is a small class of rare HMXBs that, besides the Galactic sources CI Cam, IGR J16318 − 4848, and Wd1-9, includes a couple of candidates in the Magellanic Clouds and, remarkably, two ultra luminous X-ray sources, Holmberg II X-1, and NGC 300 ULX-1/supernova imposter SN2010da (Bartlett, Clark & Negueruela 2019).

CI Cam and IGR J16318 − 4848 show variable absorbing column densities in the range 10^{23}–10^{24} cm^{-2}, intense FeKα line emission and X-ray flux variability (Bartlett et al. 2019). But while IGR J16318-4848 is bright above 20 keV (Bird et al. 2016) with some level of flaring activity (Sidoli & Paizis 2018), CI Cam has never been detected by *INTEGRAL* (Bird et al. 2016). Nevertheless, IGR J16318 − 4848 has never undergone an X-ray outburst similar to the one experienced by CI Cam in 1998: CI Cam displayed a dynamic range in excess of 500 in 8 d (from ∼5 × 10^{-8} erg cm^{-2} s^{-1} to 9 × 10^{-11} erg cm^{-2} s^{-1}), with a decline of five orders of magnitude, back to quiescence, in a few months (Belloni et al. 1999; Orlandini et al. 2000). Their X-ray luminosities cannot be determined as their distances are very uncertain. The nature of the compact object is unknown as X-ray pulsations have not been observed.

5 CONCLUSIONS

We have reported here on an *XMM–Newton* observation of AX J1714.1−3912, leading to the discovery of a remarkable new behaviour of this source. The new findings can be summarized as follows:

(i) a high intrinsic obscuration (∼1.5 × 10^{24} cm^{-2}) is observed during the flaring emission, implying a large variability of two orders of magnitude in the absorbing column density towards the source, on time-scales of years;

(ii) a prominent FeKα line emission is evident both during the flare and the unflared (quiescent) emission, with variable fluxes in the two source states;

(iii) the flare caught by *XMM–Newton* increases the source range of flux variability to ∼900, when compared to a *Chandra* observation performed two years before.

In view of these new findings, we have discussed different viable scenarios for the source nature. AX J1714.1−3912 was previously suggested to be a SFXT. The short term variability during the *XMM–Newton* observation is consistent with a SFXT nature, as well as the long-term dynamic range.

On the other hand, the *XMM–Newton* spectrum is remarkable, as no SFXT has ever shown an obscuration as large as 10^{24} cm^{-2}. This spectrum shows many similarities with those typically observed in the so-called 'highly obscured sources', a rare subclass of HMXBs with a sgB[e] companion. This might pose the SFXT identification into question and leads us to propose an alternative origin for the X–ray emission, a sgB[e] HMXB. To confirm its membership further investigations of the companion star are needed.

DATA AVAILABILITY

The *XMM–Newton* data analysed here are publicly available by means of the HEASARC (ObsID 0804300901) and the ESA archive at the link https://doi.org/10.5270/esa-nai97jb

REFERENCES

Arnaud K. A., 1996, in Jacoby G. H., Barnes J., eds, ASP Conf. Ser. Vol. 101, Astronomical Data Analysis Software and Systems V. Astron. Soc. Pac., San Francisco, p. 17

Bartlett E. S., Clark J. S., Coe M. J., Garcia M. R., Uttley P., 2013, MNRAS, 429, 1213

Bartlett E. S., Clark J. S., Negueruela I., 2019, A&A, 622, A93

Belloni T. et al., 1999, ApJ, 527, 345

Benjamin R. A. et al., 2003, PASP, 115, 953

Bird A. J. et al., 2016, ApJS, 223, 15

Boon C. M. et al., 2016, MNRAS, 456, 4111

Bozzo E. et al., 2011, A&A, 531, A130

Cardelli J. A., Clayton G. C., Mathis J. S., 1989, ApJ, 345, 245

Chaty S., Fortin F., García F., Fogantini F., 2019, Proc. IAU Symp. 346, High-mass X-ray Binaries: Illuminating the Passage from Massive Binaries to Merging Compact Objects. Kluwer, Dordrecht, p. 161

Fabian A. C., George I. M., Miyoshi S., Rees M. J., 1990, MNRAS, 242, 14P

Gaia Collaboration et al., 2016, A&A, 595, A1

Gaia Collaboration et al., 2021, A&A, 649, A1

González-Galán A., Oskinova L. M., Popov S. B., Haberl F., Kühnel M., Gallagher J., Schurch M. P. E., Guerrero M. A., 2018, MNRAS, 475, 2809

Guainazzi M., Matt G., Perola G. C., 2005, A&A, 444, 119

HI4PI Collaboration et al., 2016, A&A, 594, A116

Haberl F., 1991, A&A, 252, 272

Hickox R. C., Myers A. D., Greene J. E., Hainline K. N., Zakamska N. L., DiPompeo M. A., 2017, ApJ, 849, 53

Ibarra A., Matt G., Guainazzi M., Kuulkers E., Jiménez-Bailón E., Rodriguez J., Nicastro F., Walter R., 2007, A&A, 465, 501

Jansen F. et al., 2001, A&A, 365, L1

Koyama K., Kinugasa K., Matsuzaki K., Nishiuchi M., Sugizaki M., Torii K., Yamauchi S., Aschenbach B., 1997, PASJ, 49, L7

Kraus M., 2019, Galaxies, 7, 83

Kretschmar P. et al., 2019, New A Rev., 86, 101546

Kurucz R. L., 1993, VizieR Online Data Catalog, p. VI/39

Magdziarz P., Zdziarski A. A., 1995, MNRAS, 273, 837

Martínez-Núñez S. et al., 2017, Space Sci. Rev., 212, 59

Miceli M., Bamba A., 2018, A&A, 612, A32

Nandra K., O'Neill P. M., George I. M., Reeves J. N., 2007, MNRAS, 382, 194

Negueruela I., Smith D. M., Reig P., Chaty S., Torrejón J. M., 2006, in Wilson A., ed., Proceedings of the 'The X-ray Universe 2005', 26-30 September 2005, El Escorial, Madrid, Spain. Ed. by A. Wilson. ESA SP-604, Vol. 1. Noordwijk: ESA Publications Division, p. 165

Orlandini M. et al., 2000, A&A, 356, 163

Polletta M. et al., 2007, ApJ, 663, 81

Sguera V. et al., 2005, A&A, 444, 221

Sguera V. et al., 2006, ApJ, 646, 452

Sidoli L., 2017, in XII Multifrequency Behaviour of High Energy Cosmic Sources Workshop (MULTIF2017). Palermo, Italy, p. 52

Sidoli L., Paizis A., 2018, MNRAS, 481, 2779

Skrutskie M. F. et al., 2006, AJ, 131, 1163

Slane P., Gaensler B. M., Dame T. M., Hughes J. P., Plucinsky P. P., Green A., 1999, ApJ, 525, 357

Strüder L. et al., 2001, A&A, 365, L18

Turner M. J. L. et al., 2001, A&A, 365, L27

Uchiyama Y., Takahashi T., Aharonian F. A., 2002, PASJ, 54, L73

Verner D. A., Ferland G. J., Korista K. T., Yakovlev D. G., 1996, ApJ, 465, 487

Walter R. et al., 2003, A&A, 411, L427

Werner M. W. et al., 2004, ApJS, 154, 1

Wilms J., Allen A., McCray R., 2000, ApJ, 542, 914

Wright E. L. et al., 2010, AJ, 140, 1868

Zickgraf F. J., Wolf B., Stahl O., Leitherer C., Klare G., 1985, A&A, 143, 421

This paper has been typeset from a TeX/LaTeX file prepared by the author.